

AD-A034 056

MARYLAND UNIV COLLEGE PARK INST FOR MOLECULAR PHYSICS
INFRARED SPECTRA OF ATMOSPHERIC MOLECULES.(U)
JUN 76 W S BENEDICT

F/G 3/2

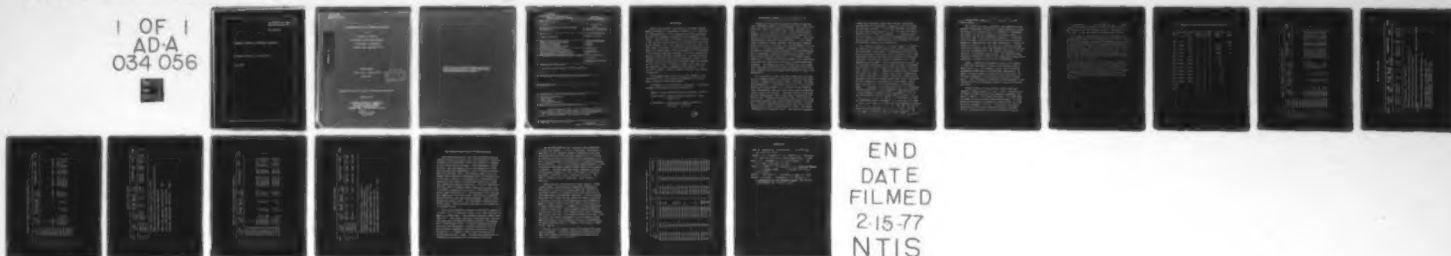
F19628-72-C-0248

UNCLASSIFIED

AFGL-TR-76-0145

NL

1 OF 1
AD-A
034 056



END
DATE
FILMED
2-15-77
NTIS

U.S. DEPARTMENT OF COMMERCE
National Technical Information Service

AD-A034 056

INFRARED SPECTRA OF ATMOSPHERIC MOLECULES

MARYLAND UNIVERSITY, COLLEGE PARK

JUNE 1976

011100
AFGL-TR-76-0145

INFRARED SPECTRA OF ATMOSPHERIC MOLECULES

BY

William S. Benedict
Institute for Molecular Physics
University of Maryland
College Park, Maryland 20742

ADA034056

FINAL REPORT

1 July 1972 - 30 June 1975

June 1976

DDC
RECEIVED
JAN 6 1977
C

Approved for public release; distribution unlimited.

Prepared for

AIR FORCE GEOPHYSICS LABORATORY
AIR FORCE SYSTEMS COMMAND
UNITED STATES AIR FORCE
HANSCOM AFB, MASSACHUSETTS 01731

REPRODUCED BY
NATIONAL TECHNICAL
INFORMATION SERVICE
U. S. DEPARTMENT OF COMMERCE
SPRINGFIELD, VA. 22161

Qualified requestors may obtain additional copies from the Defense Documentation Center. All others should apply to the National Technical Information Service.

Unclassified

SECURITY CLASSIFICATION OF THIS PAGE (When Data Entered)

REPORT DOCUMENTATION PAGE		READ INSTRUCTIONS BEFORE COMPLETING FORM
1. REPORT NUMBER AFGL-TR-76-0145	2. GOVT ACCESSION NO.	3. PERFORMER'S CATALOG NUMBER
4. TITLE (and Subtitle) INFRARED SPECTRA OF ATMOSPHERIC MOLECULES	5. TYPE OF REPORT & PERIOD COVERED Final 1 Jul 1972 - 30 June 1975	
	6. PERFORMING ORG. REPORT NUMBER	
7. AUTHOR(s) William S. Benedict	8. CONTRACT OR GRANT NUMBER(s) F19628-72-C-0248	
9. PERFORMING ORGANIZATION NAME AND ADDRESS Institute for Molecular Physics University of Maryland College Park, Maryland 20742	10. PROGRAM ELEMENT, PROJECT, TASK AREA & WORK UNIT NUMBERS 611025 76700901	
11. CONTROLLING OFFICE NAME AND ADDRESS Air Force Geophysics Laboratory Hanscom AFB, Massachusetts 01731 Monitor/Robert A. McClatchey/OPI	12. REPORT DATE June 1976	
	13. NUMBER OF PAGES 18	
14. MONITORING AGENCY NAME & ADDRESS (if different from Controlling Office)	15. SECURITY CLASS. (of this report) Unclassified	
	15a. DECLASSIFICATION/DOWNGRADING SCHEDULE	
16. DISTRIBUTION STATEMENT (of this Report) Approved for public release; distribution unlimited.		
17. DISTRIBUTION STATEMENT (of the abstract entered in Block 20, if different from Report)		
18. SUPPLEMENTARY NOTES		
19. KEY WORDS (Continue on reverse side if necessary and identify by block number) Molecular spectroscopy Water vapor Carbon dioxide Atmospheric absorption		
20. ABSTRACT (Continue on reverse side if necessary and identify by block number) Summary is given of work on new interpretation of features in the spectra of water vapor and carbon dioxide, and of the compilation of tables of lines of those and other molecules for identification of molecular lines in the infrared spectra of the earth and sunspots.		

INTRODUCTION

During the period of the contract, the AFCRL report AFCRL-TR-73-0096, by McClatchey, Benedict et al., summarizing the preparation of the extensive data tape containing over 100,000 atmospheric absorption line parameters, was issued. Activity under the contract was principally devoted to the detection and correction of inaccuracies in the tape and the report, and to the extension of the data base. For water-vapor, new higher energy levels were obtained from the umbral and flame spectra; and the analysis of the absorption in the visible region was advanced. For CO_2 , improved new spectra of Venus and Mars provided more accurate rotational constants for some of the lower vibrational levels of the isotopic forms, and additional very weak bands were measured for the first time. Progress was made in the analysis of the combination bands of methane in the 2800 cm^{-1} and 4300 cm^{-1} regions. Isotopic bands of ammonia were measured and analyzed.

The present report will give a brief summary of the above activities, with particular emphasis on the water-vapor analysis in the visible region.

In addition to the principal investigator, the following personnel were associated with the project.

James M. Krell, Research Graduate Assistant, 1972-1975.

Philip Sticha, Research Graduate Assistant, July-August 1974.

Aristophanes G. Metropoulos, Research Graduate Assistant, 1971-1973.

WATER-VAPOR ABSORPTION IN THE VISIBLE REGION

Analysis of the vibration-rotation bands of H_2O was first achieved by Mecke and collaborators (1933), who identified low-J lines in 12 bands with origins from 8807 cm^{-1} ($v_1v_2v_3 = 111$) to 17495 cm^{-1} (203). Their observational material was the telluric lines in the solar spectrum, as listed in the 1928 revision of Rowland's Table. Since that time many more lines have been identified. In the second (1966) revision by Moore, Minnaert and Houtgast, approximately 1100 lines in 16 bands are included between 541.4 and 739.2 nm. At longer wavelengths a detailed listing in the 750-1200 nm range has been published, from the Jungfraujoch data, by Swensson, Benedict, Delbouille and Roland (1970). That volume includes a tabulation of the derived energy levels for 19 vibrational states, together with a description of the general nature of the spectrum, and estimated band strengths. The AFCRL data tape includes lines and intensities calculated by the rigid-rotor approximation from those data, together with the stronger band regions at still longer wavelengths.

In the visible region, many more lines than are identified in the MMH volume can be observed and should be added to the tape, together with oxygen lines in the red. The necessary observations, covering most but not all of the visible spectrum, have been made by J. W. Brault at Kitt Peak National Observatory, and he and the writer have collaborated in the analysis of the data. The data consists of measurements of approximately 6000 lines between $13300\text{--}22900\text{ cm}^{-1}$ (440-750 nm). These were observed at very low solar angles with rapid scanning over narrow spectral ranges (~15 nm per day), recording photoelectrically onto tapes that can be computerized to yield low-sun/high-sun ratios, and thereby eliminating the Fraunhofer lines. The resulting atmospheric

spectra have excellent signal-noise ratios, and permit determination of frequencies, intensities, and line widths of quite weak features. At the most favorable conditions, the H_2O content approached 30 g cm^{-2} , and lines as weak as $.0001 \text{ cm}^{-1}/\text{g cm}^{-2}$ have been measured. An absolute basis for the intensity is achieved by intercomparisons with lines strong enough to be observed within the telescope path where the absolute humidity can be measured.

The analysis proceeds in the usual manner. As described for example in the SBDR volume, most of the strong lines, and many weaker transitions, are transitions from the well-known ground-state rotational levels to levels of the upper vibrational states that follow well-defined regularities in energy and for which the intensity relations for a rigid asymmetric rotor apply. This is particularly valid for the one strongest vibrational state among the many overlapping states within a region, namely the lowest-energy state with odd v_3 and $v_2 = 0$ or 1. Because of the odd Δv_3 , the selection rules are Type A. However, and this is increasingly the case as one moves to higher frequencies, there are many resonances due to the overlap which affect both the energies and the intensities, particularly in the weaker, Type B bands with even Δv_3 . The resonances are of three main types: (1) because of the near equality of v_1 , the symmetric stretching mode and v_3 , the asymmetric stretching mode, and a large anharmonic potential term $k_{1133}q_1^2q_3^2$, we have the Darling-Dennison resonance between pairs of levels $(v_1, v_3, J, K_a, K_c \mid v_1 \pm 2, v_3 \mp 2, K_a^e, K_c^e)$; (2) because $2v_2$, twice the deformation mode, approaches v_1 , particularly at higher v_1 and v_3 and higher K_a , we have the Fermi-Dennison resonance $(v_1, v_2, J, K_a, K_c \mid v_1 \pm 1, v_2 \mp 2, J, K_a^e, K_c^e)$; and (3) the Coriolis-type resonances $(v_3, J, K_a, K_c \mid v_3^o, J, K_a^o, K_c^e)$, which appear irregularly when the levels approach. In the above, the superscript e denotes an even parity relative to

the corresponding quantum index on the left, \circ an odd parity change.

As a result of these resonances, the intensity of the dominant vibrational transition is shared among the resonating states in a region, and it is convenient to designate each region by the total number of stretching quanta, nv , and either zero or one deformation quantum, δ . Each such region includes $(n+2)(n+1)/2$ vibrational states, mixed to a greater or less degree by the above resonances. However the states with high v_2 (≥ 4) are very weak and have not been identified; indeed, since they approach the top of the potential hill corresponding to the linear configuration, it is difficult to calculate their energy. The observed low- v_2 states can however be fitted by the conventional power-series expansions, including the D-D and F-D resonances.

Table I summarizes the present status of the system. It gives the rotationless energy of the dominant band in each region, ν_{od} , the frequency range in which observed atmospheric water-vapor lines have been assigned to, the number of bands possible and observed in each region, and the total intensity of the bands of either type in each region. Note the general regularity of the decrease in total intensity with the increasing number of quanta of the dominant band.

Further details of the analysis within the three strongest visible regions, $4v$, $4v+\delta$, and $5v$, which are also the regions which have been most carefully observed, are given in Table II. The band intensities, S_v° , listed there, are based on the relatively unperturbed levels. For such bands the strongest line should be either Q(221) or R(303), with line intensity $\approx .03 S_v^\circ$. In nearly all the type-B bands the sum of the line intensities greatly exceeds the S_v° . As mentioned in the notes to Table II, the F-D

bands with higher v_2 , at lower energy for $K_a=0$, at increasing K_a increasingly resonate with and eventually fall at higher energy than the dominant partner. The mixing of the 321, 401, 222, and 302 states is particularly striking.

The remaining unidentified lines are generally weak, and presumably arise from the higher-J levels which it has not yet been possible to confirm by combination differences or calculation, together with unsuspected perturbations from the high- v_2 levels. Note that some of these fall in other regions, for example 071 levels might overlap 301. In addition, lines of H_2O^{18} must be present, particularly in the 4v region, and a few tentative identifications have been made in 301, with $\Delta v_O \approx 35.4 \text{ cm}^{-1}$.

In the near future, Dr. Brault hopes to repeat and extend the measurements using the newly constructed FTS for more rapid coverage of the entire visible spectrum at very low sun. It is considered unlikely that a great improvement in the analysis of the regions summarized in Table II will result, but the extension to higher and lower n should be significant.

Table 1. Summary of Atmospheric Water-Vapor Absorption

Region	ν_{0d} cm^{-1}	Assigned Range cm^{-1}	Number of Bands			Total S_V^0 , $\text{cm}^{-1}/\text{g cm}^{-2}$	
			Total	$\nu_2 < 6$	obs	Type A	Type B
Rot	0	0 - 1101	1	1	1		
δ	1595	793 - 2641	1	1	1		330000
ν	3756	2658 - 4457	3	3	3	270000	16000
$\nu + \delta$	5331	4385 - 6132	3	3	3	30000	610
2 ν	7250	6271 - 8021	6	6	6	27000	2100
2 $\nu + \delta$	8807	7937 - 9590	6	6	5	1700	30
3 ν	10613	9677 - 11414	10	9	8	860	28
3 $\nu + \delta$	12151	11621 - 12846	10	9	6	48.	2.3
4 ν	13831	13185 - 14776	15	12	11	54.	1.6
4 $\nu + \delta$	15348	14907 - 16062	15	12	7	3.7	0.31
5 ν	16899	16465 - 17880	21	15	9	6.2	0.30
5 $\nu + \delta$	18393	18000 - 19000?	21	15	2	70.4	
6 ν	19781	19486 - 19858	28	18	4	70.5	70.05
6 $\nu + \delta$	21250?		28	18	1		
7 ν	22480?		36	21	1		

Table IIa, Summary of H₂O Analysis, Region 4v

$v_1 v_2 v_3$	ν_o calc cm ⁻¹	ν_o obs cm ⁻¹	No. of Lines	No. of Levels	S_o^o ν gm ⁻¹ cm	Strongest Line ν	Line S	Ident.	Notes
0 8 0	11494.9	--							
1 6 0	12614.8	--							
0 6 1	12498.9	--							
2 4 0	12614.8	--							
1 4 1	13256.25	13256 ?			0.021	13754.043	.0117	441*-322	a
0 4 2	13459.17	13448 ?	6	3	0(per t)	13748.485	.0064	431*-322	
3 2 0	13641.91	13642 ?	26	12	0(per t)	13698.303	.0497	212*-101	b
2 2 1	13642.50	13652.650	243	68	4.92	13665.814	.174	220 -221	c
2 0 2	13827.90	13828.3	210	73	0.22 ?	13890.390	.185	313*-202	d
3 0 1	13830.83	13830.922	375	102	41.8	13901.497	1.422	220 -221	c
1 2 2	13915.01	13910.8	50	22	0.16	13967.040	.0079	212 -101	
0 2 3	14068.96	14066.193	76	38	0.262	14074.342	.0081	220 -221	
4 0 0	14221.25	14221.143	205	61	1.33	14272.977	.0417	441*-432	e

Table IIa (Continued)

$v_1 v_2 v_3$	ν_o calc cm ⁻¹	ν_o obs cm ⁻¹	No. of Lines	No. of Levels	S_v^o cm gm ⁻¹	Strongest Line ν	Ident.	Notes
1 0 3	14318.90	14318.802	273	77	7.24	14371.268	.241	313 -212
0 0 4	14536.80	14536.87	71	41	0.08	14259.441	.027	414*-441

^a $K_a=6$ quite strong, ~ 60 cm⁻¹ below 301.

^bNumerous low- K_a perturbations with 221, $K_a=4$ with 301, 3.

^cCross above $K_a=4$; near exact at $K=5$, $\Delta E=58$ cm⁻¹.

^dLow- K strong borrowing, weak interaction with 301. High- K strong R branch, P very weak.

^eStrong Coriolis between 400, $K_a=4$ and 103, $K_a=3$, etc.

Total lines observed, 13274-14905 cm⁻¹, 2230.

Total lines identified, 1660 H₂O, 102 O₂.

Strongest unidentified, 13796.864, $S = .020$.

Table IIB, Summary of H₂O Analysis, Regions 4ν + δ

$\nu_1 \nu_2 \nu_3$	ν_o calc cm ⁻¹	ν_o obs cm ⁻¹	No. of Lines	No. of Levels	S_o^o ν -1 cm gm ⁻¹	Strongest Line ν	Ident.	Notes
0 9 0	12675.3	--						
1 7 0	13801.6	--						
0 7 1	13924.6	--						
2 5 0	14610.76	--						
1 5 1	14657.17	14640 ?	2	1	0 (pert)	15219.827	.0013 735*-616	
0 5 2	14865.27	--						
3 3 0	15108.95	15107 ?	3	1	0 (pert)	15414.329	.0053 432*-303	a
2 3 1	15118.33	15119.026	131	48	0.09	15418.363	.0170 432*-313	b
2 1 2	15344.58	15344.499	145	57	0.026	15418.531	.0303 414 -303	a
3 1 1	15348.11	15347.949	262	79	3.37	15345.593	.0942 220 -221	a
1 3 2	15388.25	--						
0 3 3	15540.80	--						

Table IIb (Continued)

$v_1 v_2 v_3$	ν_o calc cm ⁻¹	ν_o obs cm ⁻¹	No. of Lines	No. of Levels	S_v^o cm gm ⁻¹	Strongest Line ν S	Ident.	Notes
4 1 0	15744.55	15742.787	44	21	0.045	15938.533	.0059 532 [*] -423	c
1 1 3	15833.51	15832.757	137	55	0.51	15904.457	.0201 404 -303	c
0 1 4	16047.05	--						c

^aClose crossing resonance at $K_a=5$, $\Delta E = 90 \text{ cm}^{-1}$.

^bWeak perturbations and strong intensity borrowings from 311.

^cNo observations at high-frequency end.

Total lines observed, 14907-15 965 cm⁻¹, 980.

Total lines identified, 730 H₂O, 68 O₂.

Strongest unidentified, 15526.698, S = .0028.

Table IIc, Summary of H₂O Analysis, Region 5v

$v_1 v_2 v_3$	ν_o calc cm ⁻¹	ν_o obs cm ⁻¹	No. of Lines	No. of Levels	S_o^o cm gm ⁻¹	Strongest Line ν	Line S	Ident.	Notes
2 6 0	15961.47	--							
1 6 1	16009.88	--							
1 4 2	16223.44	--							
2 4 1	16548.06	--							
3 4 0	16811.98	16802 ?	8	3	0(per t)	16882.508	.0097	414*-303	
3 2 1	16821.53	16821.626	171	54	1.64	16825.741	.0662	220 -221	a
2 2 2	16829.50	16825.23	68	35	0.043	16903.795	.0284	505 -414	b
3 0 2	16898.61	16898.4 ?	173	60	0.08	16968.459	.0713	414*-303	b
4 0 1	16898.97	16898.828	277	78	3.53	16888.234	.098	220 -221	a
0 4 3	16977.06	--							
4 2 0	17237.26	17227.7	16	7	0.023	17280.605	.0006	212 -101	
1 2 3	17318.96	17312.54	89	37	0.052	17558.860	.0033	432*-313	
5 0 0	17458.20	17458.203	125	45	0.137	17588.729	.0066	432 -321	c

Table IIc (Continued)

$v_1 v_2 v_3$	ν_o calc cm ⁻¹	ν_o obs cm ⁻¹	No. of Lines	No. of Levels	S_o^o ν -1 cm gm ⁻¹	Strongest Line ν S	Ident.	Notes
2 0 3	17495.44	17495.517	199	61	0.684	17536.778	.0210 202 -101	
0 2 4	17531.86	--						
1 0 4	17749.02	17748.073	61	27	0.013	17816.541	.0004 414 -303	
0 0 5	17947.10	--						

^aStrong F-D mixing at low K_a . Crossing 2-3.

^bStrong F-D as above, strong borrowing.

^cStrong perturbation $K_a=3$ with $K_a=2$ of 203.

Total lines observed, 16389-17905 cm⁻¹, 1700.

Total lines identified, 1127 H₂O, 44 O₂.

Strongest unidentified line, 16879.474, $s = .0133$.

NEW CARBON DIOXIDE BANDS IN VENUS AND MARS

The infrared spectra of the light reflected from the clouds of Venus has proved a very rich source of information concerning the vibrational levels and rotational constants of the carbon dioxide molecule. The atmosphere is nearly pure CO_2 , and the combination of low temperature ($\sim 248\text{K}$) and the scattering properties of the thin haze at pressures above the 200 mbar level, which permits weak lines to be formed during multiple scatterings while the stronger lines are blocked, results in the possibility of detecting many inherently weak bands, provided observations can be made with sufficient spectral resolution. The 1967 observations with their FTS by Connes, Connes and Maillard (1969) were at an effective resolution of 0.08 cm^{-1} , and covered the frequency range $3980\text{--}8300\text{ cm}^{-1}$. The analysis of the CO_2 bands was summarized in the 1969 Atlas, and molecular constants derived from the data have been published: Connes, Connes, Benedict and Gray (1974). 209 vibrational transitions are listed there. These constants were used in the preparation of the AFCRL tape.

With a new instrument providing an effective resolution of 0.015 cm^{-1} , P. Connes and Michel (1974) have obtained new spectra. These cover a more extended frequency range ($3960\text{--}9650\text{ cm}^{-1}$). The higher resolution separates some lines that were previously blended and permits detection and measurement of some weaker lines. A careful examination of the new data, and derivation of improved constants from the more accurate frequencies, has been carried out by the writer and J. Y. Mandin of Prof. Amat's Laboratoire de Physique Moléculaire, Orsay. The detailed results will be published; we may summarize the findings as follows.

The new measurements are in general quite consistent with the 1967 spectra. In 95% of the bands, deviations of more than $.03 \text{ cm}^{-1}$ between observed frequencies and those calculated from the CCBG constants appear only at the highest observed J-values, indicating minor improvements in B' and D' and occasionally the possibility of obtaining meaningful H constants. Five of the weakest bands previously listed as observed transitions between known higher levels cannot be located. Six weak bands were given incorrect origins; the corrected values are: 626: 411IV-110II = 6149.416; 411IV-010 = 7414.507. 628: 112II-010 = 5813.48. 627: 102I-0 = 5986.13; 103I-0 = 8254.394. 638: 301II-0 = 6140.125.

Additional new transitions have been located. These include some in the previously unmeasured frequencies $8300\text{--}9650 \text{ cm}^{-1}$, others in regions where the earlier S/N was highly inferior, and others which could only be distinguished under the improved resolution. The frequencies $4810\text{--}5180 \text{ cm}^{-1}$, where the CO_2 content on Venus is so high as to result in very low returned signal were examined on spectra of Mars; most of the new bands in that range can be seen on both planets. A summary of the new transitions is given in Table III. The strongest and most important new data are the 626: 310I-0 band and its "hot" neighbors, 400I-010 and 320I-010. The analysis accounts for over 10,000 CO_2 lines, and leaves unassigned very few features which appear definitely to be planetary lines not attributable to the other molecules known to appear in this region, namely CO, HCl, and HF.

The new data in general confirm the lower-level rotational constants. The most significant inaccuracy of the older data occurs in the 628 ground state, where we now find $B = 0.368184$, $D = 1.19 \times 10^{-7}$.

Table III. New CO₂ Bands in the 1973 Connes Venus Spectra

ν_{O} cm ⁻¹	Iso.	Transition	ν_{O} cm ⁻¹	Iso.	Transition
4504.912	628	31103-00001 PR	6752.41	637	00031-00001
4527.280	636	31103-00001 R	6860.435	626	03331-03301
4673.302	628	31102-00001 PR	7414.507	626	41114-01101
4734.101	628	30014-10002	7465.298	628	40013-00001
4774.575	627	21113-01101	7526.514	627	40013-00001
4938.383	626	31101-00001 PR	7543.07	626	50014-10002
4977.464	626	32201-01101 PR	7625.751	628	40012-00001
5000.269	626	40001-01101 PR	8676.716	626	50015-00001
5151.49	626	23311-03301	8831.482	626	50014-00001
5277.151	628	01121-00001 Q	8965.225	626	50013-00001
5813.448	628	11122-01101	9137.799	626	50012-00001
6100.321	628	31113-01101	9302.144	636	20032-00001
6140.125	638	30012-00001	9320.001	626	21133-01101
6255.483	636	41101-00001 PR	9388.994	626	20033-00001
6265.203	628	31112-01101	9404.152	636	20031-00001
6374.502	636	11122-00001 PQR	9478.125	626	21132-01101
6475.820	628	11122-00001 PQR	9516.969	626	20032-00001
6515.125	636	11121-00001 PQR	9629.685	626	20031-00001
6618.561	628	11121-00001 PQR	9631.354	626	21131-01101

REFERENCES

- Mecke, R., Baumann, W., Freudenberg, K. Z. Physik 81,
313, 445, 465 (1933).
- Swensson, J. W., Benedict, W. S., Delbouille, L. and Roland,
G. Mém. Soc. Roy. Sci. Liège, Special Vol. 5 (1970).
- Moore, C. E., Minnaert, M. G. J. and Houtgast, J. Nat.
Bur. Stand. Monograph 61 (1966).
- Connes, J., Connes, P. and Maillard, J. P. Atlas des Spectres
. . . de Venus, Mars . . . Editions du C.N.R.S.,
Paris (1969).
- Connes, P. and Michel, G. Astrophys. J. 190, L29 (1974).
- Connes, P., Connes, J., Benedict, W. S. and Gray, L. D.
In Exploration of the Planetary System, Woszczyk and
Iwaniszewska, eds. (1974), p. 144.